Precise adaptation in bacterial chemotaxis through ''assistance neighborhoods''

Robert G. Endres* and Ned S. Wingreen

Department of Molecular Biology, Princeton University, Princeton, NJ 08544-1014

Edited by Howard C. Berg, Harvard University, Cambridge, MA, and approved July 12, 2006 (received for review April 17, 2006)

The chemotaxis network in *Escherichia coli* is remarkable for its sensitivity to small relative changes in the concentrations of multiple chemical signals over a broad range of ambient concentrations. Key to this sensitivity is an adaptation system that relies on methylation and demethylation (or deamidation) of specific modification sites of the chemoreceptors by the enzymes CheR and CheB, respectively. It was recently discovered that these enzymes can access five to seven receptors when tethered to a particular receptor. We show that these ''assistance neighborhoods'' are necessary for precise adaptation in a model for signaling by clusters of chemoreceptors. In agreement with experiment, model clusters composed of receptors of different types exhibit high sensitivity and precise adaptation over a wide range of chemical concentrations and the response of adapted clusters to addition/removal of attractant scales with free-energy change. We predict two limits of precise adaptation at large attractant concentrations: Either receptors reach full methylation and turn off, or receptors become saturated and cease to respond to attractant but retain their adapted activity.

Monod–Wyman–Changeux model | receptor clustering | two-state receptors | signaling

Chemotaxis allows *Escherichia coli* to sense and swim toward attractants such as amino acids and sugars and away from repellents. Temporal changes in chemical concentration are transduced to the rotary motor, leading to either straight swimming or a directional change (tumbling). The chemotaxis network is remarkably sensitive to small relative changes in chemical concentrations (ligands) over a wide range of ambient concentrations. This sensitivity relies on two features of the network: precise adaptation to persistent stimuli (1) and allosteric coupling between receptors to amplify the ligand-binding signal (2, 3). Precise adaptation of individual receptors was elegantly explained by Barkai and Leibler (4) with a model of activity-dependent receptor modification. However, the Barkai and Leibler (BL) model does not directly extend to allosterically coupled receptors. We reconcile this apparent contradiction by making use of the recent observation that the methylating and demethylating enzymes CheR and CheB do not act on single receptors but on groups of five to seven receptors, so-called ''assistance neighborhoods'' (5).

In the *E. coli* chemotaxis network, there are five types of chemoreceptors bound in the cytoplasmic membrane: the high-abundance Tsr and Tar, which specifically bind serine and aspartate, and the low-abundance Tap, Trg, and Aer. The receptors form homodimers, which in turn assemble into mixed trimers of dimers (6–8). Receptors cluster at the cell poles (9), facilitated by the linker protein CheW and the histidine kinase CheA (10), which phosphorylates the response regulator CheY. Phosphorylated CheY binds to the rotary motors and induces clockwise rotation of the flagella and tumbling of the cell. When CheA is inactive, CheY is unphosphorylated; motors rotate counterclockwise; and cells swim straight.

Both ligand binding and receptor methylation affect the activity of CheA. For example, an increase of attractant inhibits CheA activity, but subsequent methylation of specific receptor modification sites returns CheA activity to its original level. There are four main modification sites common to all receptors, and these are expressed by the cell as amino acid residues QEQE (where Q is glutamine and E is glutamate). Glutamines can be deamidated by CheB to glutamates, which can be reversibly methylated/demethylated by CheR/CheB. The high-abundance receptors Tar and Tsr have a 35-amino acid-long tether at their C terminus to which CheR or CheB can bind (11) for facilitating effective chemotaxis (12, 13). *In vitro* measurements show that once a CheR or CheB is tethered, the enzyme can act on five to seven nearby receptors defining an assistance neighborhood (5). There is strong evidence that receptors *in vivo* form interacting clusters several times larger than these observed assistance neighborhoods. Specifically, *in vivo* FRET measurements of the receptor sensitivity (14) and Hill coefficients (15) indicate coupled clusters of 10–20 receptors (15–18).

In this work, we use a simple mixed-cluster Monod–Wyman–Changeux (MWC) (16, 17, 19) model of strongly coupled receptors to account for experimental dose–response curves of adapted cells measured by using *in vivo* FRET (14). Importantly, we present a mechanism for precise adaptation of receptor clusters based on assistance neighborhoods. Our model can explain the observed broad range of sensitivity without invoking changes in ligand-binding affinities. Furthermore, we identify two distinct limits of adaptation at high attractant concentration: receptors either saturate and hence stop responding, or receptors fully methylate and hence stop adapting. We propose that these two limits can be predicted from the behavior of fully methylated $CheB^-$ mutants.

Model

MWC Model. We assume that an individual receptor homodimer of type r (where $r = a$ and s for Tar and Tsr, respectively) can be described as a two-state receptor (20), being either on or off. Such a two-state receptor has four possible free-energy values: (*i*) on without ligand-bound $E^{\rm on}_{r(m)}$; (*ii*) on with ligand-bound $E^{\rm on}_{r(m)} - \log([L]/K^{\rm on}_r)$; (*iii*) off without ligand-bound $E^{\rm off}_r$; and (*iv*) off with ligand-bound $E^{\rm off}_r - \log([L]/K^{\rm off}_r)$, where $[L]$ is the ligand concentration in the medium, and m is the number of methyl groups attached to the receptor dimer ($m = 0, \ldots, 8$). The dissociation constants for ligand in the on and off states are $K^{\rm on}_r$ and $K^{\rm off}_r$, respectively, and are assumed to be independent of methylation level (17). All energies are expressed in units of the thermal energy k_BT. In our model, methylation favors the on state of a receptor dimer by lowering $E^{\rm on}$, whereas attractant binding favors the off state, i.e., $K^{\rm off} < K^{\rm on}$ (the opposite inequality applies for repellents). Fig. 1 shows graphically the energetics of a single receptor as a function of attractant concentration and degree of methylation. The curve for the off

Conflict of interest statement: No conflicts declared.

This paper was submitted directly (Track II) to the PNAS office.

Abbreviations: BL model, Barkai and Leibler model; MWC model, Monod–Wyman–Changeux model.

*To whom correspondence should be addressed. E-mail: rendres@princeton.edu.

www.pnas.org/cgi/doi/10.1073/pnas.0603101103

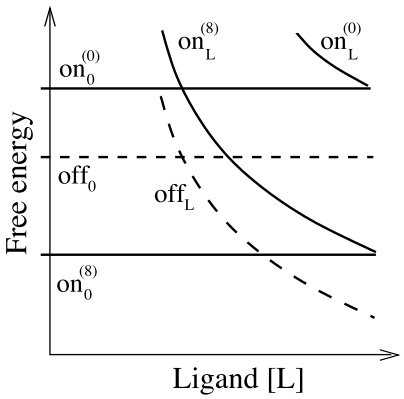

Fig. 1. Representative energy-level diagram for a single receptor as a function of attractant (ligand) concentration. Shown are the free energies of the on states (solid lines) with and without bound ligand, on_L and on_0, and similarly for the off states (dashed lines). For clarity, only the free energies of the fully demethylated (0) and fully methylated (8) on states are shown. By convention, the free energies of the off states do not depend on receptor methylation.

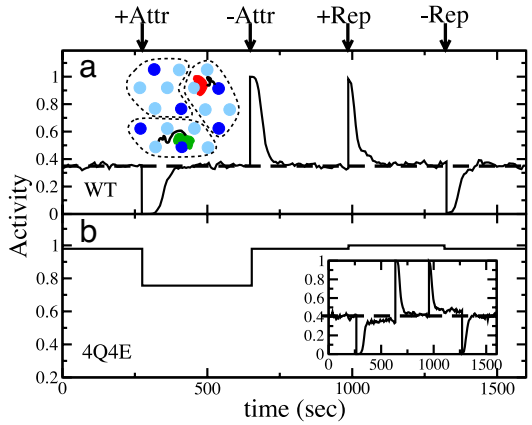

Fig. 2. Theoretical response of receptor activity to addition/removal of attractant (Attr) and repellent (Rep) for mixed clusters of adapting (WT) receptors (*a*) and nonadapting half-methylated or amidated receptors (*b*) (4Q4E). Attr: 100 μM MeAsp for WT and 50 μM MeAsp at 50 μM ambient MeAsp for 4Q4E. Rep: 100 μM $NiCl_2$ for WT and 4Q4E. (*a Inset*) Schematic cluster of receptors with tethered CheR (green) and CheB (red) acting on assistance neighborhoods (within dashed lines). Receptor colors are as follows: high-abundance Tsr (light blue) and Tar (dark blue). (*b Inset*) Same simulation as *a* but without employing assistance neighborhoods.

state with ligand off_L may lie below or above the curve for the fully methylated on state with ligand $on_L^{(8)}$, with distinct consequences to be explored below. Within this model, the combined free energy of the two on states is $f_{r(m)}^{\rm on} = E_{r(m)}^{\rm on} - \log(1 + [L]/K_r^{\rm on})$ and for the two off states is $f_r^{\rm off} = E_r^{\rm off} - \log(1 + [L]/K_r^{\rm off})$.

In the MWC model (15, 19), two-state receptors form clusters with all receptors in a cluster either on or off together. We used a variant of the MWC model in which clusters are composed of mixtures of two types of receptors, in particular Tar and Tsr (16–18). At equilibrium, the probability that an MWC cluster will be active is

$$p_{\rm on} = \frac{e^{-F^{\rm on}}}{e^{-F^{\rm on}} + e^{-F^{\rm off}}} = \frac{1}{1 + e^{F}}, \qquad [1]$$

where $F = F^{\rm on} - F^{\rm off}$, and where $F^{\rm on/off}$ is the free energy of the cluster to be on/off as a whole. Hence, the average activity per receptor in the cluster is $A = p_{\rm on}$. For a cluster composed of n_a Tar receptors and n_s Tsr receptors, the total free-energy difference is $F = \Sigma_{i=1}^{n_a} f_a(m_i) + \Sigma_{j=1}^{n_s} f_s(m_j)$, which is just the sum of the individual free-energy differences between the receptor on and off states

$$f_{r(m)} = f_{r(m)}^{\rm on} - f_r^{\rm off} = \varepsilon_{r(m)} + \log\left(\frac{1 + [L]/K_r^{\rm off}}{1 + [L]/K_r^{\rm on}}\right). \qquad [2]$$

Here, the methylation state of the receptor enters only via the "offset energy" $\varepsilon_{r(m)} = E_{r(m)}^{\rm on} - E_r^{\rm off}$. In practice, we use the same offset energies $\varepsilon_{r(m)}$ for both Tar and Tsr receptors. Those receptor offset energies are as follows, where m is the number of methylated (or amidated) modification sites in a receptor homodimer (17): $\varepsilon_{r(0)}$, 1.0; $\varepsilon_{r(1)}$, 0.5; $\varepsilon_{r(2)}$, 0.0; $\varepsilon_{r(3)}$, −0.3; $\varepsilon_{r(4)}$, −0.6; $\varepsilon_{r(5)}$, −0.85; $\varepsilon_{r(6)}$, −1.1; $\varepsilon_{r(7)}$, −2.0; $\varepsilon_{r(8)}$, −3.0. The generalization of Eq. **2** for binding multiple types of ligand is given in supporting information, which is published on the PNAS web site.

Adaptation Model. We model adaptation along the lines of the BL model (4) by assuming that the demethylating enzyme CheB works only on active receptors and that the methylating enzyme CheR works only on inactive receptors (21–23). To achieve precise adaptation within the MWC model, we assume the methylating and demethylating enzymes CheR and CheB work on groups of six receptors (assistance neighborhoods) (5). Each assistance neighborhood is fully contained within an MWC cluster, so that all receptors in a neighborhood are active or inactive together. Methylation/demethylation is assumed to be equally likely for each available modification site within the assistance neighborhood.

Simulation Details and Parameters. We model a mixed cluster of 18 receptors, composed of 6 Tar and 12 Tsr receptors, in line with the experimental ratio. Inside the cluster, we define for simplicity three nonoverlapping assistance neighborhoods of six receptors, each containing two Tar and four Tsr receptors (Fig. 2*a Inset*). We use Eq. **1** to calculate the equilibrium probability for a cluster with particular methylation levels of its receptors to be active at a particular ligand concentration. We use the methylation-dependent offset energies from above and the following dissociation constants: $K_a^{\rm off} = 0.02$ mM and $K_a^{\rm on} = 0.5$ mM for MeAsp binding by Tar; $K_s^{\rm off} = 100.0$ mM and $K_s^{\rm on} = 10^6$ mM for MeAsp binding by Tsr (as in ref. 17); $K_s^{\rm off} = 0.01$ mM and $K_s^{\rm on} = 1.0$ mM for serine binding by Tsr; $K_a^{\rm off} = 100.0$ mM and $K_a^{\rm on} = 10^6$ mM for serine binding by Tar; and $K_r^{\rm off} = 0.5$ mM and $K_r^{\rm on} = 0.05$ mM for $NiCl_2$ binding by both Tar ($r = a$) and Tsr ($r = s$).

Because methylation and demethylation rates are slow compared with ligand binding and unbinding, we model methylation/demethylation kinetics explicitly. The time evolution of the methylation and demethylation of receptors in the cluster is simulated with the stochastic but exact Gillespie algorithm (24). The algorithm requires three random numbers. The first determines which assistance neighborhood gets methylated with rate $\gamma_R(1 - p_{\rm on})$ or demethylated with rate $\gamma_B p_{\rm on}$. The second decides which modification site in the assistance neighborhood is methylated/demethylated. The third, r_3, is needed to correctly increment the simulation time. r_3 is chosen with a uniform probability on the interval [0, 1], and the time is increased according to $\delta t = 1/\{3[\gamma_R(1 - p_{\rm on}) + \gamma_B p_{\rm on}]\ln(1/r_3)\}$. We used methylation/demethylation rates $\gamma_B = 2\gamma_R$ leading to a steady-state activity of 1/3. The rate constant $\gamma_R = 0.1$/s was chosen to set a convenient time scale. All adaptation simulations are averaged over 100 independent runs.

Results

Receptor Response: Comparison with FRET Experiments. To compare with *in vivo* FRET experiments (14), we simulated the response

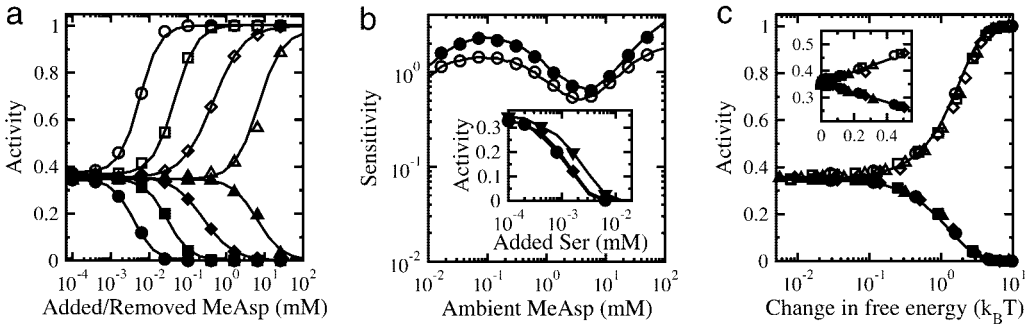

Fig. 3. Theoretical response of WT, adapting receptors to steps of MeAsp at different ambient concentrations. (*a*) Activity immediately after step change in concentration of MeAsp after complete adaptation to ambient concentrations 0 (circle), 0.1 (square), 0.5 (diamond), and 5 (triangle) mM. Additional MeAsp was added (filled symbols) and then removed after adaptation (open symbols) in a sequence of steps of increasing size. (*b*) Dependence of the response sensitivity, defined as $(\Delta A/A)/(\Delta[L]/[L])$, where A is activity, on increases in the concentration of MeAsp of 10% (filled circles) and 50% (open circles), as a function of the ambient concentration. (*b Inset*) Activity immediately after step change in concentration of serine after complete adaptation to ambient concentrations of MeAsp: 0 (filled circle), 10 mM (filled diamond), and 100 mM (filled triangle). Curves in *a* and *b* are to guide the eye. (*c*) Data from *a* plotted as a function of the absolute value of free energy change upon addition/removal of attractant. (*c Inset*) Same data for small free-energy changes plotted on a linear scale; slopes are $\pm 0.2/k_BT$. Curves in *c* are calculated by using the free energy model (see supporting information).

of receptor cluster activity to step changes of ligand concentration. In Fig. 2, we show the averaged response of 100 independent clusters, each consisting of 6 Tar and 12 Tsr homodimers (the nominal *in vivo* ratio), to addition and subsequent removal of attractant as well as repellent. In Fig. 2, for wild-type (WT) receptors, the initial response is followed by precise adaptation back to the steady-state activity. In Fig. 2*b*, for receptor homodimers fixed at half methylation or amidation (4Q4E) there is no adaptation; the initial activity is nearly maximal, and response to attractant, and particularly to repellent, is reduced compared with WT, in line with experiment (figure 1b of ref. 14).

The BL model yields precise adaptation for single receptors (4) but not for allosterically coupled receptor clusters. In the BL model, the demethylation rate depends only on receptor activity, not on ligand concentration or methylation level. This model yields precise adaptation as long as receptors do not become fully methylated or demethylated. However, for receptors in strongly coupled MWC clusters, the methylation level of a single receptor is only weakly correlated with cluster activity and hence with methylation/demethylation rates. The result is a broad distribution of methylation levels including fully methylated and fully demethylated receptors and, consequently, imprecise adaptation of cluster activity (Fig. 2*b Inset*). In contrast, our extension of the BL model to include assistance neighborhoods within MWC clusters does yield precise adaptation, as shown in Fig. 2*a*. Specifically, assistance neighborhoods increase the ladder of methylation levels from 8 for a single receptor homodimer to 48 for an assistance neighborhood of 6 receptors. This increase of methylation levels allows CheR and CheB to function at saturation without encountering fully methylated or demethylated conditions. Moreover, within an assistance neighborhood, all available sites are modified with equal probability, providing a "return force" on individual receptor methylation levels (more available sites implies greater probability of modification) and narrowing the methylation-level distribution. (Additional analysis, including dependence on the size of assistance neighborhoods, can be found in Fig. 7 and in supporting information.)

By using our assistance-neighborhood adaptation model, we studied the chemotactic response of WT receptors adapted to different ambient concentrations of attractant. We found close agreement with experiment (cf. figure 3 a–c of ref. 14). As in experiment, the larger the ambient concentration, the larger the step change in attractant required for a given immediate change of activity. In contrast, receptors preadapted to MeAsp stay maximally sensitive to serine until Tsr receptors start binding MeAsp, ≈100 mM MeAsp (see Fig. 3*b Inset*). In Fig. 3*b*, the sensitivity (defined as the ratio of the fractional change of output to the fractional change of input) shows two peaks, which are explored below. Experimental *in vivo* FRET data corresponding to our simulation results in Fig. 3*a* were previously shown to collapse to a single curve when plotted as a function of the free-energy change of receptors (17). In our mixed-cluster MWC model, the activity of a cluster depends only on the total free-energy difference between its on and off states. Precise adaptation implies that methylation returns this free-energy difference very close to its steady-state value. Therefore, after adaptation, the immediate response to addition or removal of MeAsp depends only on the additional free-energy change due to the change in attractant concentration (see supporting information). In Fig. 3*c*, we show the collapse of the activity data from Fig. 3*a* when plotted as a function of the change in cluster free energy.

Two Peaks of Response Correspond to Tar and Tsr Affinities for MeAsp. To better understand the sensitivity shown in Fig. 3*b*, we consider $\Delta A/(\Delta[L]/[L])$, which stays well defined even when the activity (A) vanishes through failure of adaptation. Fig. 4*a* shows that WT, adapted receptors (solid line) respond over a broad range of MeAsp concentration, with two peaks. Also shown is the result for nonadapting receptors with fixed methylation (or amidation) levels. These receptors respond only over narrow ranges of concentration, with the range of response shifting to higher concentration with increasing methylation level. Neglecting fluctuations, the response can be factored as

$$\frac{\Delta A}{\Delta[L]/[L]} \xrightarrow{\Delta \to 0} \frac{dA}{d\log([L])} = \frac{dA}{dF}\frac{dF}{d\log([L])}, \qquad [3]$$

where F is the free-energy difference between the on and off states of the cluster as a whole. Fig. 4*b* shows that the two peaks in sensitivity derive from the second factor, $dF/d\log([L])$, which applies equally to WT and nonadapting receptors and depends only on the number of Tar and Tsr receptors and their ligand dissociation constants (see supporting information). The two peaks in receptor sensitivity correspond, respectively, to the ranges over which Tar and Tsr bind MeAsp. The remaining first factor dA/dF, shown in Fig. 4*c*, is constant for the WT (assuming perfect adaptation) and is peaked for nonadapting receptors.

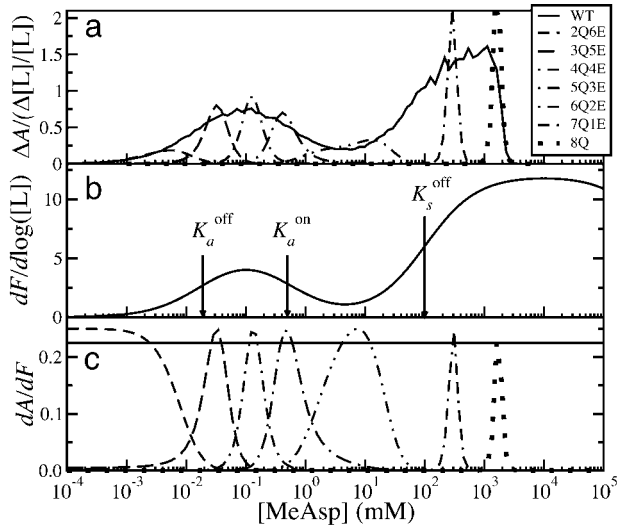

Fig. 4. Two peaks of receptor response to MeAsp. (*a*) Theoretical receptor response $\Delta A/(\Delta[L]/[L])$ for mixed clusters of receptors as a function of ambient MeAsp concentration ($[L]$) for $\Delta[L]/[L] = 10\%$. Curves show responses of adapted (WT) and nonadapting (xQyE, where *x* and *y* are the number of glutamines/methyl groups and glutamates, respectively) receptors. Plotted are averages over 100 independent simulations for clusters of 18 receptors, 6 Tar, and 12 Tsr. (*b* and *c*) Analytical results for single mixed cluster. (*b*) Methylation independent $dF/d\log([\text{MeAsp}])$; also shown are the MeAsp dissociation constants for Tar (*a*) and Tsr (*s*) receptors. (*c*) dA/dF; WT is assumed to adapt for all MeAsp concentrations. Key applies to *a* and *c*.

Two Limits of Adaptation. There are two distinct limits of adaptation, as shown in Fig. 5 for a single receptor. At low ligand concentration, changes in methylation can adjust the total free-energy difference between the on and off states of the receptor to achieve precise adaptation. At large ligand concentration, one of two possibilities occurs. (*i*) As shown in Fig. 5*a*, the off state with ligand bound is the lowest free-energy state. The receptor is inactive, because, even when fully methylated, the on state is disfavored. (*ii*) Alternatively, as shown in Fig. 5*b*, the fully methylated on state with ligand bound is the lowest free-energy state. The methylation level can still be adjusted to achieve precise adaptation. However, because the receptor is fully saturated, it will not respond to further addition of ligand. These arguments can be extended to clusters of receptors. At large ligand concentrations, either

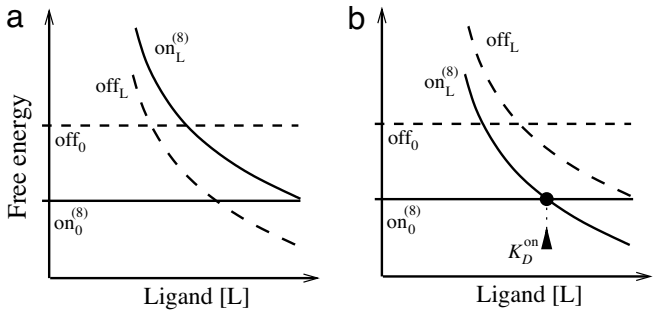

Fig. 5. The two limits of adaptation, illustrated for a single receptor. (*a*) Receptor turns off at large attractant concentration if the off state with ligand becomes the lowest free-energy state. (*b*) Receptor retains adapted activity but ceases to respond to ligand if the fully methylated on state with ligand becomes the lowest free-energy state. The curve labels are the same as in Fig. 1. The arrow indicates K_D^{on}, i.e., the concentration at which a receptor in the on state is occupied by attractant 50% of the time.

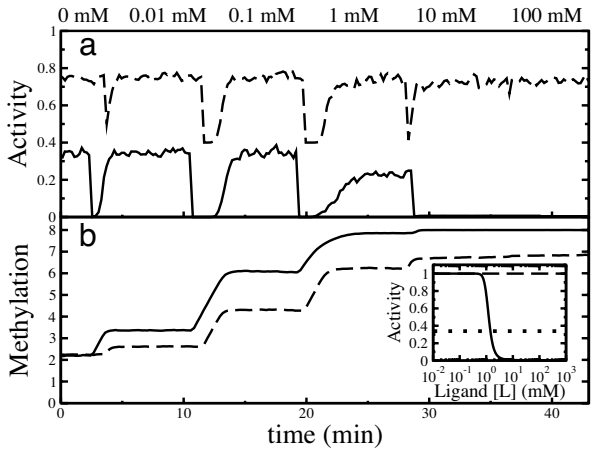

Fig. 6. Adaptation of a homogeneous cluster of 18 receptors for different values of K^{off}: 0.018 (solid line) and 0.06 (dashed line) mM. The remaining parameters correspond to Tar and MeAsp values. (*a*) Response of receptor activity to progressive step increases in attractant concentration (0–100 mM). Solid curve is raised vertically by 0.4. (*b*) Corresponding average receptor methylation levels. (*Inset*) Activity as a function of attractant concentration for fully methylated receptors. The steady-state activity of adapted receptors is indicated by the dotted line.

the off state with ligand fully bound is the lowest free-energy state and activity is lost, or the fully methylated on state with ligand fully bound is the lowest free-energy state, and activity freezes at the adapted value.

As an example of the two limits of adaptation, we study the response of a homogeneous cluster of 18 identical receptors to progressive step increases of attractant. Fig. 6 shows two activity curves and corresponding averaged methylation levels for receptors with different values of K^{off}. The receptors with the smaller K^{off} (solid curve) start binding ligand at relatively low concentrations. Consequently, methylation increases rapidly, and the receptors become fully methylated before they become saturated with ligand above K^{on} (= 0.5 mM). Further addition of ligand reduces the activity of these receptors to zero (Fig. 5*a*). In contrast, the receptors with the larger K^{off} value (dashed curve) start binding ligand at relatively large concentrations. Methylation increases slowly, and the receptors saturate before becoming fully methylated. This process allows the receptors to maintain their adapted activity, but they stop responding to further addition of ligand (Fig. 5*b*). Which of the two limits of adaptation occurs depends on the activity of the fully methylated receptors at high ligand concentration: If low, receptors turn off; if high, receptors stop responding (see Fig. 6 *Inset*).

The limit of adaptation of a heterogeneous cluster depends on the fraction of ligand-binding receptors. For example, for a mixed cluster of Tar and Tsr receptors with the Tars saturated by MeAsp, increasing the number of Tars favors the off state (limit of adaptation by loss of activity), whereas increasing the number of Tsrs favors the on state (limit of adaptation by loss of response).

Discussion

The chemosensing system of *E. coli* is remarkable for its ability to adapt precisely over a wide range of external attractant or repellent concentrations (1, 14, 25). The BL model yields precise adaptation for single receptors (4, 26) but not for receptor clusters (Fig. 2*b Inset*). In the BL model, the demethylation rate depends only on receptor activity, not on ligand concentration or methylation level. This characteristic leads to precise adaptation, provided CheR (CheB) does not encounter fully methylated (demethylated) receptors. However, when receptors are strongly

coupled in clusters, the cluster activity only poorly reflects the methylation level of individual receptors, leading to a broad distribution of methylation levels, including fully methylated or demethylated receptors, and hence to imprecise adaptation.

We have shown that an extension of the BL model to include assistance neighborhoods (5) does yield precise adaptation for strongly coupled clusters (Fig. 2). Our use of assistance neighborhoods follows the recent observation by Li and Hazelbauer (5) that a single CheR or CheB protein tethered to a receptor has a range of, respectively, seven or five receptors in the immediate vicinity. In our model, CheR and CheB can modify any available site in the assistance neighborhood. Assistance neighborhoods effectively increase the ladder of methylation levels such that CheR and CheB rarely encounter fully methylated or demethylated conditions. The result is essentially perfect adaptation.

At large attractant concentrations, our model predicts two distinct limits of adaptation: Either receptors reach full methylation and stop adapting (turn off), or receptors become saturated and cease to respond to attractant but retain their adapted activity. Which limit occurs can be predicted from the behavior of a fully methylated mutant (e.g., receptors expressed with four glutamates in a $CheB^-$ background). If the fully methylated mutant becomes inactive at large attractant concentrations, then WT cells will stop adapting; if the mutant stays active, then WT cells will stop responding but stay precisely adapted (cf. Fig. 6*a* and *b Inset*).

Our model explains not only precise adaptation, but also the observed broad range of sensitivity to MeAsp. Because there are fewer Tar receptors than Tsr receptors, the Tars become saturated by MeAsp before clusters reach full methylation, because the Tsrs provide extra methylation sites. Hence, the clusters retain their adapted activity, but the Tars cease to respond to MeAsp above $K_a^{on} = 0.5$ mM. Subsequently, the range of sensitivity to MeAsp is extended to >0.5 mM through the low-affinity binding of MeAsp by Tsr receptors (Fig. 4).

Whereas adaptation to MeAsp and aspartate is precise over many orders of magnitude, adaptation to serine is not precise over such a large range (1). In our model, the prevalence of Tsr receptors leads to clusters becoming fully methylated before the Tsr receptors are saturated by serine. Additional binding of serine to Tsr receptors turns clusters off at >1 mM serine (see supporting information). Note, however, that the large fraction of Tsr receptors leads to high sensitivity at low serine concentrations. Physiologically, this sensitivity advantage may outweigh the disadvantage of imprecise adaptation at large serine concentrations.

Previous adaptation models of coupled two-state receptors have been described in refs. 27–29. In these models, fully methylated receptors need to be fully active, and fully demethylated receptors need to be fully inactive to achieve precise adaptation. These conditions become difficult to impose for strongly coupled receptors. In contrast, the use of assistance neighborhoods of six receptors leads to essentially perfect adaptation, even for very strongly coupled receptors (e.g., the MWC model). Assistance neighborhoods are "evolvable" insofar as increasing neighborhood size continuously improves the precision of adaptation up to approximately six receptors but give little improvement beyond that, as shown in Fig. 7.

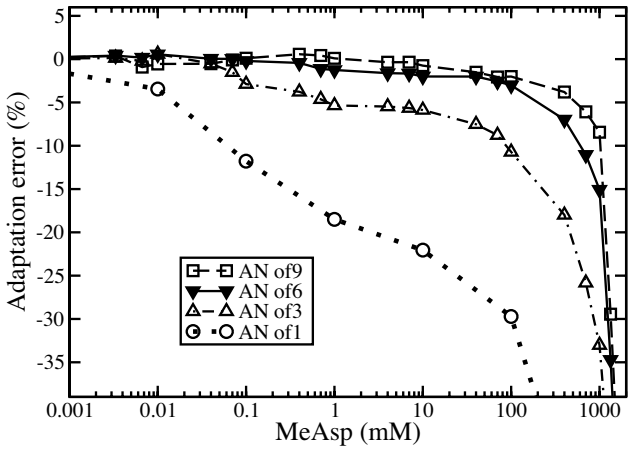

Fig. 7. Adaptation error $[A([MeAsp]) - A(0)]/A(0)$, where A is the time-averaged receptor activity, for increasing assistance neighborhood (AN) sizes of 1, 3, 6, and 9 receptors, for a mixed cluster of 6 Tar and 12 Tsr receptors. Each AN has the same Tsr:Tar ratio of 2:1, except when the AN size is 1.

The proposed importance of assistance neighborhoods for precise adaptation can be tested experimentally. First, elimination of assistance neighborhoods by removal of the receptor C terminus pentapeptide binding site for CheR and CheB should dramatically reduce the range of concentrations over which cells can adapt precisely. [In such an experiment, CheR and CheB would need to be overexpressed to compensate for their reduced activities (30).] Second, assistance neighborhoods imply cross-methylation of noncognate receptors during adaptation. Early *in vivo* experiments showing transient cross-methylation (31) might be profitably revisited in light of receptor assistance neighborhoods.

We thank Fred Hughson, Yigal Meir, Tom Shimizu, Monica Skoge, Victor Sourjik, and Jeffry Stock for valuable suggestions. This work was supported by the Human Frontier Science Program.

1. Berg, H. C. & Brown, D. A. (1972) *Nature* **239,** 500–504.
2. Bray, D., Levin, M. D. & Morton-Firth, C. J. (1998) *Nature* **393,** 85–88.
3. Duke, T. A. & Bray, D. (1999) *Proc. Natl. Acad. Sci. USA* **96,** 10104–10108.
4. Barkai, N. & Leibler, S. (1997) *Nature* **387,** 913–917.
5. Li, M & Hazelbauer, G. L. (2005) *Mol. Microbiol.* **56,** 1617–1626.
6. Kim, K. K., Yokota, H. & Kim, S. H. (1999) *Nature* **400,** 787–792.
7. Ames, P., Studdert, C. A., Reiser, R. H. & Parkinson, J. S. (2002) *Proc. Natl. Acad. Sci. USA* **99,** 7060–7065.
8. Studdert, C. A. & Parkinson, J. S. (2004) *Proc. Natl. Acad. Sci. USA* **101,** 2117–2122.
9. Maddock, J. R. & Shapiro, L. (1993) *Science* **259,** 1717–1723.
10. Liberman, L., Berg, H. C. & Sourjik, V. (2004) *J. Bacteriol.* **186,** 6643–6646.
11. Barnakov, A. N., Barnakova, L. A. & Hazelbauer G. L. (1999) *Proc. Natl. Acad. Sci. USA* **96,** 10667–10672.
12. Lai, W. C. & Hazelbauer, G. L. (2005) *J. Bacteriol.* **187,** 5115–5121.
13. Li, M. & Hazelbauer, G. L. (2006) *Mol. Microbiol.* **60,** 469–479.
14. Sourjik, V. & Berg, H. C. (2002) *Proc. Natl. Acad. Sci. USA* **99,** 123–127.
15. Sourjik, V. & Berg, H. C. (2004) *Nature* **428,** 437–441.
16. Mello, B. A. & Tu, Y. (2005) *Proc. Natl. Acad. Sci. USA* **102,** 17354–17359.
17. Keymer, J. E., Endres, R. G., Skoge, M., Meir, Y. & Wingreen, N. S. (2006) *Proc. Natl. Acad. Sci. USA* **103,** 1786–1791.
18. Skoge, S., Endres, R. G. & Wingreen, N. S. (2006) *Biophys. J.* **90,** 4317–4326.
19. Monod, J., Wyman, J. & Changeux, J. P. (1965) *J. Mol. Biol.* **12,** 88–118.
20. Asakura, S. & Honda, H. (1984) *J. Mol. Biol.* **176,** 349–367.
21. Stock, J. B. & Koshland, D. E. (1981) *J. Biol. Chem.* **256,** 10826–10833.
22. Terwilliger, T. C., Wang, J. Y. & Koshland, D. E., Jr. (1986) *J. Biol. Chem.* **261,** 10814–10820.
23. Shapiro, M. J., Panomitros, D. & Koshland, D. E. (1995) *J. Biol. Chem.* **270,** 751–755.
24. Gillespie, D. T. (1977) *J. Phys. Chem.* **81,** 2340–2361.
25. Alon, U., Surette, M. G., Barkai, N. & Leibler, S. (1999) *Nature* **397,** 168–171.
26. Yi, T-.M., Huang, Y., Simon, M. I. & Doyle, J. (2000) *Proc. Natl. Acad. Sci. USA* **97,** 4649–4653.
27. Shimizu, T. S., Aksenov, S. V. & Bray, D. (2003) *J. Mol. Biol.* **329,** 291–309.
28. Mello, B. A. & Tu, Y. (2003) *Biophys. J.* **84,** 2943–2956.
29. Mello, B. A., Shaw, L. & Tu, Y. (2004) *Biophys. J.* **87,** 1578–1595.
30. Li, M. & Hazelbauer G. L. (2004) *J. Bacteriol.* **186,** 3687–3694.
31. Sanders, D. A. & Koshland, D. E., Jr. (1988) *Proc. Natl. Acad. Sci. USA* **85,** 8425–8429.